Next Materials 12 (2026) 102300

Contents lists available at ScienceDirect

Next Materials

journal homepage: www.sciencedirect.com/journal/next-materials

Research article

Fungal chitosan thin film from palm oil mill effluent as sustainable piezoelectric biomaterial

Alia Tasnim Hazmi [a], Farah B. Ahmad [a,*], MH Maziati Akmal [b], Aliza Aini Md Ralib [c], Fathilah Ali [a]

[a] Department of Chemical Engineering & Sustainability, Faculty of Engineering, International Islamic University Malaysia, Kuala Lumpur 53100, Malaysia
[b] Department of Science in Engineering, Faculty of Engineering, International Islamic University Malaysia, Kuala Lumpur 53100, Malaysia
[c] Department of Electrical and Computer Engineering, Faculty of Engineering, International Islamic University Malaysia, Kuala Lumpur 53100, Malaysia

ARTICLE INFO

Keywords:
Aspergillus
Chitin
Chitosan
Fungi
Plackett–Burman
Palm oil mill effluent (POME)
piezoelectric

ABSTRACT

Chitosan extracted from fungal biomass could be used as sustainable and biodegradable piezoelectric material. This study aims to fabricate the fungal chitosan thin films using palm oil mill effluent (POME) for piezoelectric applications. POME is a waste from the palm oil industry and used as the sustainable carbon substrate in cultivating the fungi. The cultivation of fungi *Aspergillus oryzae* using POME was optimized for maximum yield of fungal biomass using Plackett-Burman (PB) design. PB design shows that the highest fungal biomass was produced at 17.5 g/L from the cultivation medium composed of KNO_3, $CaSO_4{\cdot}2\,H_2O$, yeast extract and POME. Chitosan is extracted from fungal biomass through extraction and deacetylation of chitin using alkali and organic acid treatment. Different organic acids were investigated in fabricating chitosan thin film using solvent casting technique. Formic acid showed promising results compared to the other acids and further used in fabricating POME-derived fungal chitosan thin films. The physical, chemical, electrical, and structural properties of the fungal chitosan thin film were observed. The mechanical quality factor (Q_m) of the POME-derived fungal chitosan thin film using formic acid as the solvent was 11.9, with dissipation factor (tan δ) of 0.083, which demonstrated its potential as piezoelectric biomaterial from sustainable source.

1. Introduction

Piezoelectric effect occurred as the electric polarization present in the material as any stress being applied to it [1]. Piezoelectric application is extensive, where it is used in energy harvesting, sensors, and biomedical devices [2]. A condition must be met for the piezoelectric effect to be induced, where it will only occur in a material that has non-centrosymmetric crystalline structure [3]. Piezopolymers, such as poly(vinylidene fluoride) (PVDF) and piezoceramics, such as lead zirconate titanate (PZT) have been used as efficient piezoelectric materials [1]. PVDF, is a well-known piezoelectric polymer that has crystalline structure, resulting in piezoelectric properties [3]. However, some piezoceramics and piezopolymers are highly toxic. For instance, the presence of lead oxide in PZT, which renders it non-biocompatible to humans as wearable devices or medical applications.

Biomaterials that exhibited piezoelectricity, such as biopolymer, are nontoxic and biocompatible to be used in various applications especially in tissue engineering [4]. A few studies demonstrated piezoelectricity in chitosan [5–7]. Chitosan and chitin are the second most abundant natural polysaccharide [8]. Chitosan is a natural polymer obtained from deacetylation of chitin, where it is composed of linear polysaccharide of β-1,4-*D*-glucosamine [7]. Chitosan can be extracted from the shells of crab, shrimp, and prawn, through a few conventional processes such as demineralization, deproteinization, decolouration and deacetylation of chitin [6]. The degree of deacetylation of the chitin should reach about 50%, to ensure that chitin were successfully converted into chitosan [5]. The extraction of chitosan from non-food sources, like fungal biomass, ensures sustainability of chitosan production. Chitosan has been successfully extracted from *Aspergillus* fungi [7,9,10]. Fungi could be cultivated on various carbon substrates, typically pure sugars like glucose. For upscaling the cultivation of fungi, the use of pure sugars is not economical. Opportunity exists to utilize low-cost industrial waste, like palm oil mill effluent (POME), as a cheap cultivation medium and carbon substrate due to high composition of organic carbon and nutrients of POME [11].

POME is the wastewater from the oil palm processing [12]. It is

* Corresponding author.
E-mail address: farahahmad@iium.edu.my (F.B. Ahmad).

https://doi.org/10.1016/j.nxmate.2026.102300
Received 23 August 2025; Received in revised form 22 April 2026; Accepted 16 May 2026
Available online 30 May 2026

considered as pollutant due to its composition of different suspended materials and high level of biochemical oxygen demand (BOD) and chemical oxygen demand (COD) [13]. POME itself is not harmful, but could render environmental issues when it is dumped into the river without proper guidelines, due to its extremely high BOD and COD values. The amount of POME produced per year in palm oil producing country like Malaysia is massive, which could be quite challenging and costly to properly manage and treat this waste [14]. In Malaysia, the ponding system (i.e. anaerobic method) has been mainly used in treating the palm oil wastewater due to its low operating cost and low energy requirement [15,16]. This system also has drawbacks where it requires a large area to set up the system and also it takes longer to start–up the system [15]. Utilizing POME as the cultivation media for fungal cultivation could improve POME treatment system by potentially integrating with palm oil biorefinery [11,13]. Fresh POME contains some minerals, like Fe, Zn, P, Mg, Ca and K, as well as organic acids, making it suitable to be used as carbon source [17]. The utilization of POME as microbial cultivation or fermentation medium is a type of bioremediation of POME for higher value product synthesis that can lead to significant reduction of COD or BOD [11].

Using POME as the carbon source helped in reducing the economic cost of cultivation and decreasing the burden of treating the wastewater from palm oil industry. However, there are no studies yet on the cultivation of fungi in POME for chitosan production. The focus of this study is to fabricate a thin film using chitosan as biomaterial and to evaluate its piezoelectric properties. Although there are no studies on POME-derived fungal chitosan as piezoelectric material, there are studies that employed commercial chitosan for piezoelectricity [5,6,18]. The use of POME as the cultivation medium in this study for fungal chitosan production falls under United Nation Sustainable Development Goal (UN SDG) 12, which is to ensure sustainable consumption and production patterns. The utilization of POME for the fungal cultivation would subsequently improve the wastewater management and sustainability practice in palm oil industry.

2. Materials and methods

2.1. Materials

The fungi that used in this study is *Aspergillus oryzae* from UKM Culture Collection Center, Malaysia. Palm oil mill effluent (POME) was provided by Tennamaram Palm Oil Mill (Sime) and stored at 4 °C. It was used in fungal cultivation alongside KH_2PO_4 (Merck, 3 N), K_2HPO_4 (Merck, anhydrous), $MgSO_4{\cdot}7H_2O$ (Merck, ≥98%), $CaSO_4{\cdot}2H_2O$ (Merck, ≥99%), KNO_3 (Sigma-Aldrich, ≥99%), $ZnSO_4{\cdot}7H_2O$ (Merck, 99%), $NaNO_3$ (Sigma-Aldrich, 99%), $FeCl_3{\cdot}6H_2O$ (Merck, 97%), yeast extract (Sigma-Aldrich) and glucose (Sigma-Aldrich, 99%). Potato dextrose agar (PDA) powder (Millipore) was also used during the cultivation. The extraction of fungal chitosan involved the usage of NaOH (Sigma-Aldrich, ≥98%), acetic acid (Sigma-Aldrich, ≥99%), and HCl (Sigma-Aldrich, 37%). Formic acid (Sigma-Aldrich, ≥95%), acetic acid (Sigma-Aldrich, ≥99%, lactic acid (Sigma-Aldrich, ≥85%), tartaric acid (Sigma-Aldrich, ≥99.5%), and citric acid (Sigma-Aldrich, ≥99.5%) were used in fabrication of chitosan thin films.

2.2. Fungal strain and cultivation

Potato dextrose agar (PDA) powder was used to prepare the solid medium, where 9.75 g of the PDA powder was mixed with 250 mL of distilled water. The mixture was autoclaved at 190 °C for about 20 min. After the medium was cooled, the solid medium was then poured into the petri dishes. After that, the petri dishes were kept inside the chiller until further use for fungi subculturing.

The medium was prepared to culture the strain in a liquid medium for the cultivation process. The compositions of the basic medium are (by g/L), KH_2PO_4 (0.875), K_2HPO_4 (0.375), $MgSO_4.7H_2O$ (1.0 – 1.5), $CaSO_4.2H_2O$ (0.1 – 0.5), $MnSO_4.4H_2O$ (0.005 – 0.05), NaCl (1.25), $ZnSO_4.7H_2O$ (1.0 – 1.5), $FeCl_3.6H_2O$ (1.0–1.5) and glucose (2.5), modified from Nilsson & Bjurman [19]. The mixture was mixed and then autoclaved for 22 min at 190 °C. The cultivation was performed for 15 days.

Table 1
Parameters for Plackett–Burman (PB) design on the composition of the medium, where POME is palm oil mill effluent.

Compound	Range
KNO_3	0 – 1.5 g/L
$FeCl_3.6H_2O$	0 – 1.5 g/L
$MgSO_4.7H_2O$	0 – 1.5 g/L
$ZnSO_4.7H_2O$	0 – 1.5 g/L
$CaSO_4.2H_2O$	0 – 1.5 g/L
Glucose	0 – 25 g/L
Yeast extract	0 – 5 g/L
POME	0 – 250 mL

During the cultivation of the fungi, a small volume of cultivation medium sample was taken every day. The samples taken were analysed using high-performance liquid chromatography (HPLC; Agilent) to observe the glucose consumption during the cultivation. This was done to observe how much of the glucose provided in the cultivation media used during the growth phase of the fungi. The glucose consumption was calculated from the area under the graph obtained from the HPLC analysis. The mobile phase used was deionized water with glucose used as the standard (2%, 4%, 6%, 8%, and 10%). The column used was YMC-Triart C18. Chemical Oxygen Demand (COD) analysis was also performed on the medium samples according to the standard method using a HACH high range kit [11,20].

2.3. Screening of media composition via Plackett-Burman method for fungal biomass

Plackett–Burman (PB) design was used for screening the necessary carbon source and nutrients for the fungal cultivation of *A. oryzae*. The composition of NO^{3-}, Fe^{2+}, Mg^{2+}, Zn^{2+}, Ca^{2+}, glucose, yeast extract and POME, were varied to find the best media composition for the growth of *A. oryzae* on POME medium (Table 1) [19]. The design of experiment is shown in Table 2, where the response of the experimental design is fungal biomass concentration, obtained from each run involving eight factors at maximum and minimum levels with three centre points.

2.4. Extraction of fungal chitosan

Cultivation of fungi was performed by inoculating fungal spores from fungi subculture into cultivation medium consisted of KNO_3, $CaSO_4.2H_2O$, yeast extract and POME, respectively at 1.5, 1.5, 5 g/L and 250 mL.

After 15 days of cultivation, the harvested fungal biomass was extracted based on our previous study [10], where alkaline and dilute organic acid technique was used. The biomass was deproteinized using 4 M NaOH with ratio of 1:40 *w/v* at 90 ℃ for 3 h. The alkali-insoluble material (AIM) was centrifuged at 6000 rpm for 15 min and washed using the distilled water to achieve neutral pH. Chitosan was extracted from the AIM by using 10% *v/v* acetic acid with ratio of 1:40 *w/v* on a rotary shaker for 6 h at 200 rpm. The mixture was filtered, where residue of acid insoluble was discarded after filtration is done. The filtrate was adjusted to pH 9 using 4 M NaOH solution. The solution was centrifuged and washed with distilled water and dry overnight at 60 ℃.

2.5. Fabrication of chitosan thin films

Solvent casting was chosen as a method to fabricate the chitosan thin film. 0.5 g of chitosan powder (pure chitosan or fungal chitosan) and

Table 2
The factors (medium composition (g/L for A-F and H, mL for G)) for the design of experiment using Plackett–Burman (PB) and the response, which is fungal biomass concentration (g/L).

Run	Factor								Response
	A: KNO_3 (g/L)	B: $FeCl_3.6H_2O$ (g/L)	C: $MgSO_4.7H_2O$ (g/L)	D: $ZnSO_4.7H_2O$ (g/L)	E: $CaSO_4.2H_2O$ (g/L)	F: Glucose (g/L)	G: POME (mL)	H: Yeast extract (g/L)	Fungal biomass (g/L)
1	0	0	0	1.50	0	25.0	250	0	10.08
2	0	1.50	1.50	0	1.50	25.0	250	0	0
3	0	0	1.50	0	1.50	25.0	0	5.0	0
4	0	0	0	0	0	0	0	0	0
5	0	1.50	1.50	1.50	0	0	0	5.0	12.53
6	0	1.50	0	1.50	1.50	0	250	5.0	2.62
7	0.75	0.75	0.75	0.75	0.75	12.5	125	2.5	12.76
8	0.75	0.75	0.75	0.75	0.75	12.5	125	2.5	13.38
9	0.75	0.75	0.75	0.75	0.75	12.5	125	2.5	15.16
10	1.50	1.50	1.50	0	0	0	250	0	14.01
11	1.50	0	1.50	1.50	1.50	0	0	0	0
12	1.50	0	1.50	1.50	0	25.0	250	5.0	16.30
13	1.50	1.50	0	1.50	1.50	25.0	0	0	3.50
14	1.5	1.5	0	0	0	25.0	0	5	6.54
15	1.5	0	0	0	1.5	0	250	5	17.50

50 mL of acid (acetic acid, formic acid, citric acid, tartaric acid or lactic acid) were stirred in a beaker at 90 °C for 3 h [9]. After the chitosan has completely dissolved, the solution was poured into a petri dish and left overnight to dry at 60 °C [21].

2.6. Chemical and physical characterization of chitosan thin films

Chemical properties of chitosan thin film were analysed using X-ray diffraction (XRD), Fourier-transform infrared spectroscopy (FTIR) (INVENIO, Bruker, USA) and degree of deacetylation (DDA). The crystallinity of the thin films and the crystallinity index (*CrI%*) was observed using XRD (PANalytical) analysis where the reading was taken from 5° until 40°. The continuous scan was used on all thin films. FTIR analysis was done to identify chemical functional groups and DDA of fungal chitosan to validate the efficiency of extraction method. The sample was ground with diluents to fine powder before going through the analysis. The result was in absorbance, where the range was taken from 400 cm^{-1} to 4000 cm^{-1}. DDA measures the degree of conversion of chitin into chitosan based on acetyl group removal. DDA was measured based on Eq. 1, using FTIR spectra of chitosan sample, where A_{1655} is the absorbance at wavenumber 1655 cm^{-1} and A_{3450} is the absorbance at wavenumber 3450 cm^{-1} [22].

$$DDA = 100 - \frac{\left(\frac{A_{1655}}{A_{3450}} \times 100\right)}{1.33} \quad (1)$$

The surface morphology of the thin film was studied using field emission scanning electron microscope (FESEM) analysis (Hitachi SU8020). The sample was kept dry and sub-coating was done as the sample is a polymer. The accelerating voltage used was 1 kV and the images were taken at 30,000x. Tensile strength of thin film was tested using the tensile test using Univeral Tensile Machine (Shimadzu) to determine the break point of the thin films. The thin films were cut into rectangular (4 cm×2 cm). With speed at 10 mm/min, the stretching of the thin films was observed until the thin films break. DSC experiments were performed on a DSC822e (Mettler Toledo, USA). Transmission Electron Microscope (TEM) (Talos L120C) analysis was performed on POME-derived fungal chitosan thin film with resolution of 0.2 nm at 120 kV. Piezoresponse Force Microscopy (PFM) (NX-10, Park Systems) analysis was conducted on POME-derived fungal chitosan thin film with scan range of 15 μm, resolution of 0.015 nm, position detector noise of 0.03 nm (bandwidth: 1 kHz) and resonant frequency of > 9 kHz. Gwyddion software was used for data visualization and analysis.

2.7. Electrical characterization of chitosan thin films

Piezoelectricity of chitosan thin film in this study was measured indirectly via mechanical quality factor (Q_m) and dissipation factor (tan δ). The measurement can be undertaken using the LCR meter, a type of electronic test equipment that measure the inductance (L), capacitance (C), and resistance (R) of a component. Q_m is one of the important parameters for piezoelectricity that can determine the energy loss from the material (Eq. 2) [23]. Tan δ is defined as the ratio of imaginary ε and real ε, where ε is permittivity (Eq. 3) [1].

$$Q_m = \frac{1}{R}\sqrt{\frac{L}{C}} \quad (2)$$

$$\delta = \frac{1}{Q_m} \quad (3)$$

Effective inverse piezo sensitivity, or effective piezoelectric coefficient, d_{eff} (Eq. 4), is based on the combination of the components of the piezoelectric tensor to describe the resulting response of the PFM cantilever to the applied voltage along the z-axis [24], where A_{em} is the amplitude of the electromechanical strain driving the cantilever tip and V_{tip} is the applied voltage.

$$d_{eff} = \frac{A_{em}}{V_{tip}} \quad (4)$$

2.8. Biological characterization of chitosan thin films

Biological property of chitosan thin films was assessed through biodegradability test that was carried out for a month. The thin films were cut into rectangles and weighed before the biodegradability test. Four setups for this experiment were chosen where one setup is for control, where the chitosan thin films were left in normal room temperature. The second setup was submerging the thin films in effective microorganism (EM) solution, the third setup was burying the thin films in soil and the fourth setup involved burying the thin films in soil where the EM has been mixed with the soil. The film was washed and dried [25], followed by the measurement of the weight loss of the thin films, calculated using Eq. 5.

$$Weight\ loss = \frac{weight\ of\ original\ films - weight\ of\ residual\ films}{weight\ of\ residual\ films} \times 100 \quad (5)$$

Anti-microbial activity test was conducted using *Staphylococcus aureus* (Gram-positive bacteria) and *Escherichia coli* (Gram-negative

Table 3
(a) Analysis of variance for the Plackett-Burman design on the fungal biomass concentration as the response. (b) Regression model diagnostics from analysis of variance of the model.

(a)

Source	Sum of squares	Degree of freedom	Mean square	*F*-value	*P*-value	
Model	384.14	7	54.88	9.00	0.0080	significant
A-KNO_3	41.89	1	41.89	6.87	0.0395	significant
D-$ZnSO_4.7H_2O$	51.30	1	51.30	8.42	0.0273	significant
E-$CaSO_4.2H_2O$	115.83	1	115.83	19.00	0.0048	significant
G-POME	64.13	1	64.13	10.52	0.0176	significant
Curvature	142.05	1	142.05	23.30	0.0029	significant
Residual	36.58	6	6.10			
Lack of Fit	33.47	4	8.37	5.39	0.1625	not significant
Pure Error	3.10	2	1.55			
Cor Total	562.76	14				

(b)

Modeling statistics	**Values**
R^2	0.9131
Adjusted R^2	0.8116
Standard deviation	0.1665
Mean	2.29
Coefficient of variation (%)	7.28

bacteria). Chitosan thin films and ampicillin (control) were placed onto Petri dishes with Mueller–Hinton agar that were inoculated with bacteria suspensions, followed by incubation at 37 °C for 24 h [26]. After the incubation, the diameter of the area of the microbial inhibition zone was measured [26].

3. Results and discussion

3.1. Fungi cultivation with POME medium only

Fungi cultivation was performed on POME medium only as the sole carbon source and nutrient for the cultivation of fungi strain *Aspergillus oryzae*. Despite using only POME medium with no addition of nutrients and other carbon and nitrogen sources, fungal biomass can be harvested from the medium, with 18.9 g/L yield. This shows that the fungi can grow even in POME medium as POME itself contains carbon sources (glucose and organic acids) and many minerals and can act as cultivation medium for growing fungi *A. oryzae* [11,17].

3.2. Screening of cultivation medium for fungal cultivation using Plackett-Burman design

It is of the utmost importance that maximum biomass can be harvested from fungal cultivation on POME which would be further used in the extraction of chitosan and fabrication of piezoelectric thin films. Plackett–Burman (PB) design was used for screening experiments where the main effects were confounded by two factor interactions. PB design was used in this study to optimize the fungal biomass on the cultivation on POME media. The influence of eight factors which were NO^{3-}, Fe^{2+}, Mg^{2+}, Zn^{2+}, Ca^{2+}, glucose, yeast extract and POME was investigated in 15 runs, with three center points. Center points detect curvature in the response and estimate variability without having to replicate all the corner points [27]. Center points are runs where numeric factors are set midway between their low and high levels [27], where in this experimental design it is at Runs 7–9. Table 2 shows the results of the cultivation using different composition of nutrients.

Table 3 (a) shows the analysis of variance (ANOVA) of the design. The Model *F*-value of 9.00 implies the model is significant. There is only a 0.80% chance that an *F*-value this large could occur due to noise. *P*-values is the values of *Prob>F*, where statistical significance at a *P*-value of 0.05 or 5% with confidence interval (CI) are frequently calculated at a confidence level of 95% [28,29]. *P*-values less than 0.0500 indicate model terms are significant, where the model could be used for further design guide [30]. ANOVA shows that KNO_3 (*A*), $ZnSO_4.7H_2O$ (*D*), $CaSO_4.2H_2O$ (*E*), POME (*G*) are significant model terms, which shows that only these components are crucial factors in the media preparation for further optimization of fungal biomass concentration (X_{fungi}). The concentration of fungal biomass could be predicted from the concentration of the nutrients with Eq. 6, where *A* is referring to the concentration (g/L) of KNO_3, *B* is for $FeCl_3.6H_2O$, *C* is for $MgSO_4.7H_2O$, *D* is for $ZnSO_4.7H_2O$, *E* is for $CaSO_4.2H_2O$, *F* is for glucose, *H* is for yeast extract and X_{fungi} is for fungal biomass; and *G* is for POME volume in mL. The results show the highest fungal biomass with the combination of KNO_3, $CaSO_4.2H_2O$, POME, and yeast extract in the medium.

$$X_{fungi} = 6.07 + 1.87A + 2.27D - 3.40E + 0.83F + 2.31G + 0.8417H + 1.90AG \quad (6)$$

From Table 3 (b), the R^2 value of the design is 0.9131 with adjusted R^2 at 0.8116, in which the model could be used for further design guide [30,31]. Adjusted R^2 indicates the amount of variation around the mean explained by the model, adjusted for the number of parameters in the model [29,32]. Standard deviation associated with this experiment is 0.1665 g/L. Coefficient of variation calculates the standard deviation expressed as a percentage of the mean [32]. The coefficient of variance obtained in this study at 7.28% indicates low variability, as it is below 10% [33].

Fig. 1(a) shows the plot of predicted versus actual for the fungal biomass concentration that was determined by Eq. 6. The plot shows good agreement of the predicted fungal biomass to the actual fungal biomass. Fig. 1(b) depicts the plot of residuals versus predicted for the fungal biomass. The plot shows that the residuals are structureless and do not display any obvious pattern. The undesirable pattern in the plot is when the form of megaphone or outward-opening funnel was exhibited, which is due to the increase of variance, as the magnitude of the predicted values increases [29]. Therefore, this statistical analysis demonstrated that the mathematical model is correct, and the assumptions are satisfied, where the model is reliable for predicting the fungal biomass produced from the cultivation on POME.

Pareto chart (Fig. 2) displays the estimated effect of variables on fungal biomass concentration as the response. Bonferroni limit is threshold of the significant variables means any effect that extends from that is potentially important, whereas *t*-value is the absolute values of the estimated effects divided by the standard error [34]. It draws two horizontal reference lines on the chart, where the effects that lie between these lines are deemed moderately important [34]. The chart shows that nine of the eleven factors have major influence on fungal biomass concentration. The concentration of $CaSO_4.2H_2O$ was the most significant to fungal biomass concentration with negative effect,

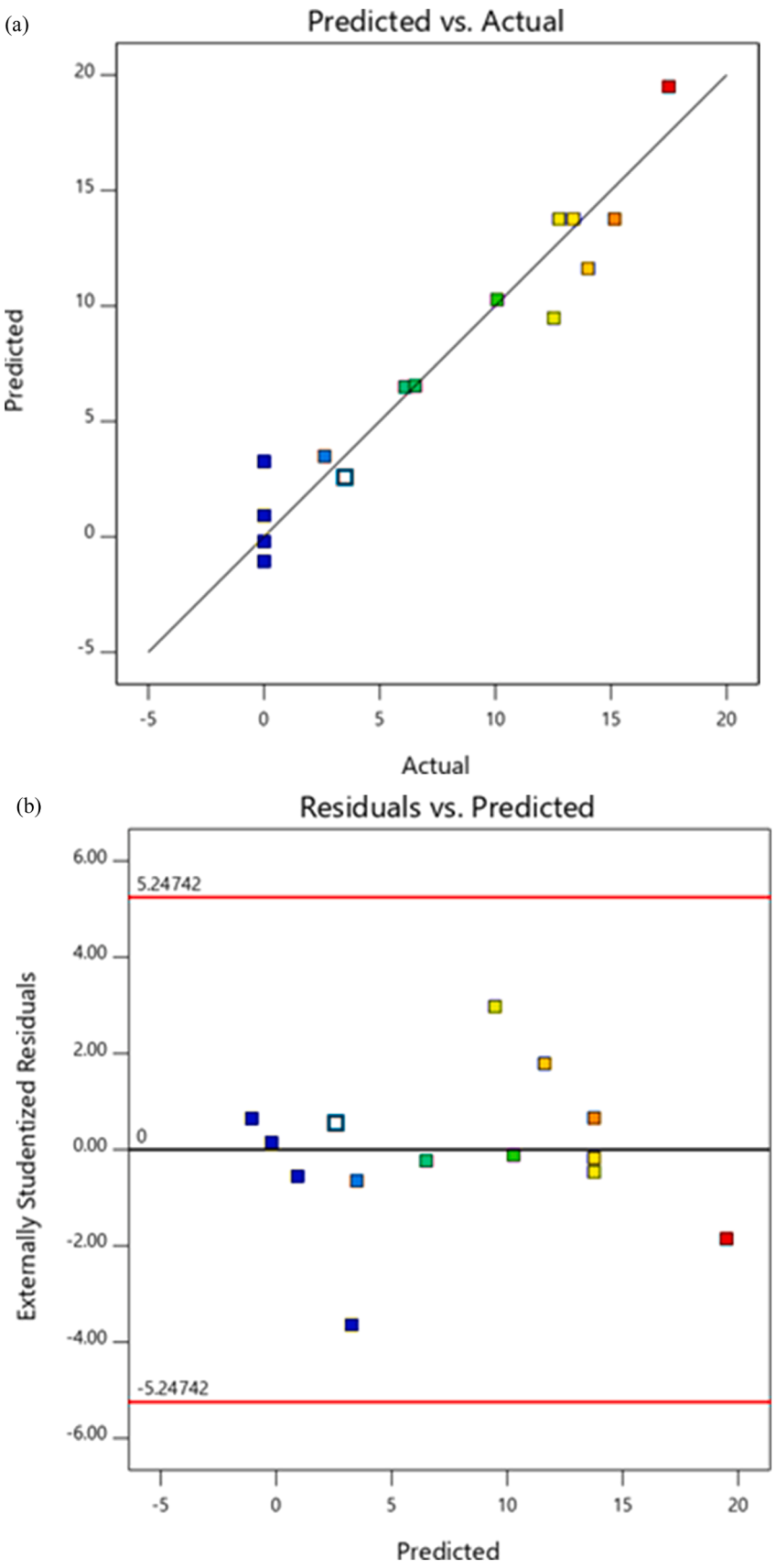

Fig. 1. (a) Plot of predicted versus actual of the fungal biomass. (b) residuals versus predicted of fungal biomass.

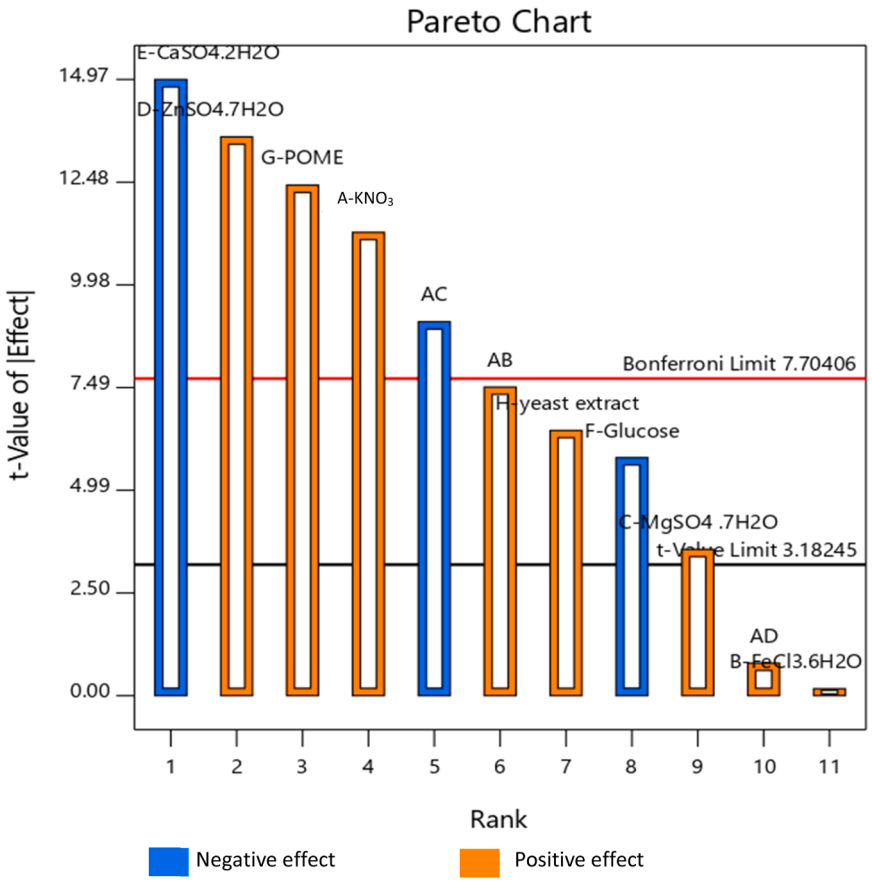

Fig. 2. Pareto chart for fungal biomass concentration from PB design.

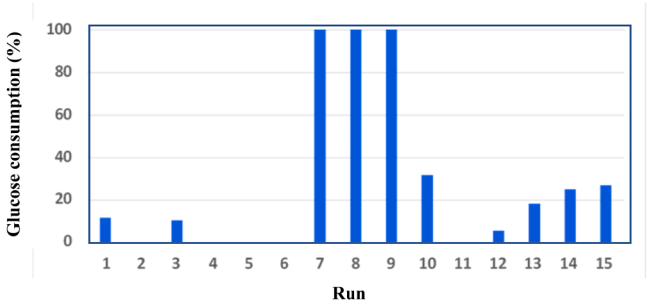

Fig. 3. Glucose consumption (%) during fungal cultivation from PB design.

followed by the concentration of $ZnSO_4.7H_2O$, POME and KNO_3 with positive effect. $ZnSO_4$ is an inorganic salt that is commonly used in the production of edible fungi, for the purpose of promoting growth, nutrient synthesis, and disease prevention [35]. $ZnSO_4$ was reported to exhibit the fastest mycelial growth rate amongst other inorganic salts with vigorous growth of *Phallus dongsun* fungi [36]. Elemental sulphur is critical in signalling, redox balance, gene expression promotion and the maintenance of fundamental metabolic processes of cells [36]. The use of KNO_3 as the nitrogen source resulted on faster mycelial growth rate of *Phallus dongsun*, in comparison to peptone, yeast powder, yeast extract, carbamide, NH_4Cl and $(NH_4)SO_4$ [36]. The concentration of yeast extract and $MgSO_4.7H_2O$ is moderately significant with positive effect to fungal biomass concentration, whereas the concentration of $FeCl_3.6H_2O$ is not significant to the biomass concentration. This could be due to the existence of magnesium and iron in POME [17].

From the PB design, only Runs 1, 2, 3, 7, 8, 9, 12, 13 and 14 were provided with glucose as supplementary carbon source. The glucose was consumed in all those runs that produced fungal biomass, which excludes Runs 2 and 3 (Fig. 3). The highest glucose consumption occurred during runs 7, 8, and 9, which were the center points of the design. In the cultivation with the highest fungal biomass produced (Run 15), there was glucose consumption measured even though it was not supplied with glucose during cultivation. This glucose consumption could be attributed to the presence of residual glucose in POME (8 g/L) [11]. Therefore, fungi has the ability to grow with POME as the media, as in the cultivation of Runs 10 and 15. For Run 2 and 3, even though there were respectively both glucose and POME, and glucose only in the cultivation media, the cultivation did not produce fungal biomass, possibly due to the lack of nitrogen source in the media [37]. Nitrogen sources are crucial for the growth of mycelia [37].

From the cultivation based on the PB design, Run 15 resulted in the highest fungal biomass concentration, even without supplemented with glucose as the carbon source. The high growth in Run 15 was possibly contributed by the other carbon sources present in POME such as residual palm oil, glucose and organic acids [17]. *A. oryzae* has been reported to have the capacity to assimilate and grow in non-conventional carbon sources such as glycerol, acetic acid and xylose [38,39].

Chemical oxygen demand (COD) analysis was performed on Run 15, where COD of the medium before cultivation is 30,420 ppm, and COD was reduced by 37% after the fungal cultivation to 21,030 ppm. This result shows that *A. oryzae* is promising for bioremediation of POME, as has been demonstrated in other studies on COD reduction of POME by the fungi [11].

3.3. *Effect of different acid solvents on chemical and physical properties of chitosan thin film*

Pure chitosan thin films were prepared using different acid solvents

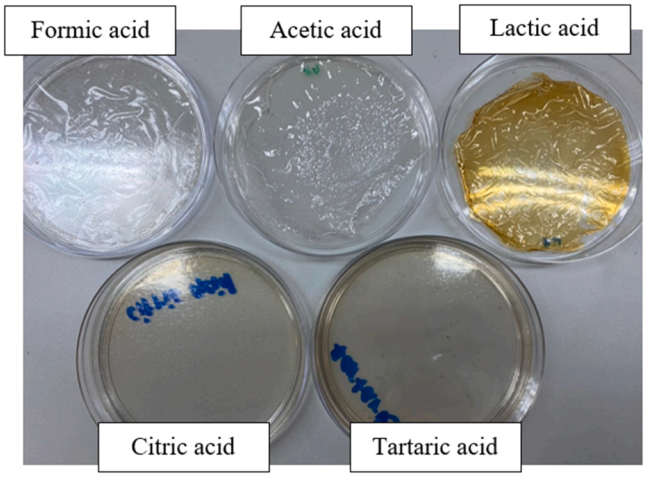

Fig. 4. Pure chitosan thin films fabricated using solvent casting method, prepared using different acid solvent.

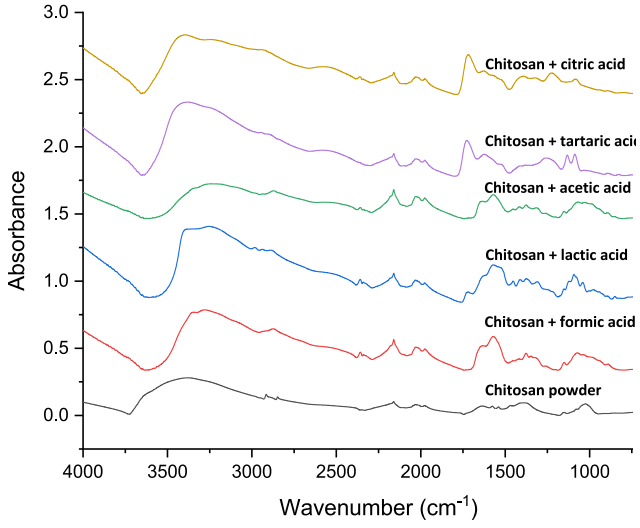

Fig. 5. FTIR spectra of pure chitosan thin films using different acid solvents and chitosan powder.

(acetic acid, formic acid, citric acid, tartaric acid and lactic acid) to optimize the solvent casting conditions for the fabrication of the film. The optimized parameters would be used to fabricate thin films from POME-derived fungal chitosan. Fig. 4 shows that only chitosan thin film from acetic and formic acid are colorless, whereas the use of other organic acids resulted on some coloration for the chitosan thin film.

Fourier transform infrared spectroscopy (FTIR) analysis was performed on the pure chitosan films prepared with five different acid solvents (Fig. 5), in order to assess the effect of different solvents on the functional groups of the films. All thin films and chitosan powder showed wide absorption bands around 3000–3600 cm^{-1}, showing the stretching of hydroxyl groups and amino groups of carbohydrate ring [21]. Absorption band at 942–1118 cm^{-1}, indicating the characteristic of polysaccharide [40]. The amide II band in formic acid, lactic acid, acetic acid, tartaric acid, and citric acid were 1481 cm^{-1}, 1478 cm^{-1}, 1476 cm^{-1}, 1476 cm^{-1}, and 1478 cm^{-1} respectively. The amide II band indicated the content of NH_3^+ groups in the thin films. Higher frequency of amide II band showed lower *pKa*. The interaction between chitosan and acid increased as the *pKa* of acid decreased [21]. Among all the acids, formic acid reported to have the lowest *pKa* at 3.75 [41]. Defined peak between 1500 and 1760 cm^{-1} is missing from the spectra of

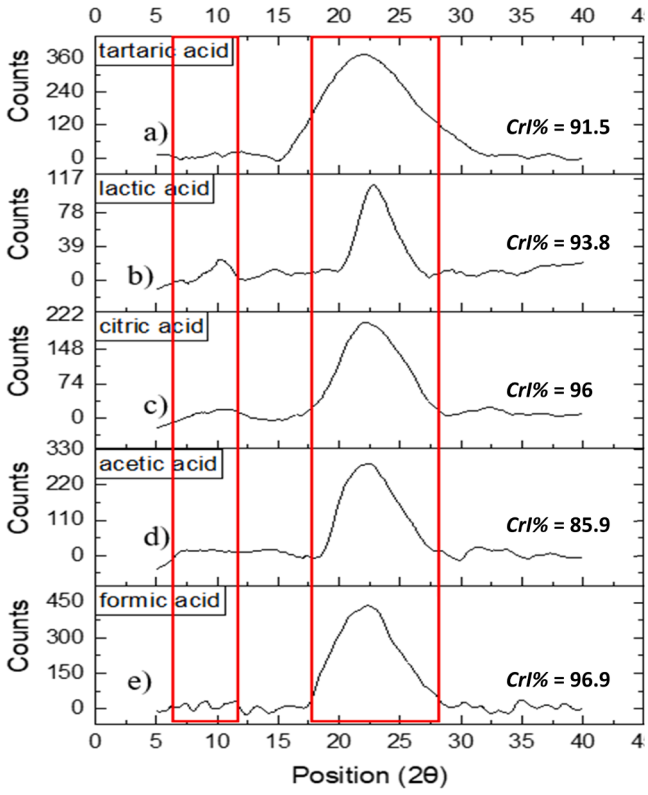

Fig. 6. XRD spectra of pure chitosan thin films using different acid solvents.

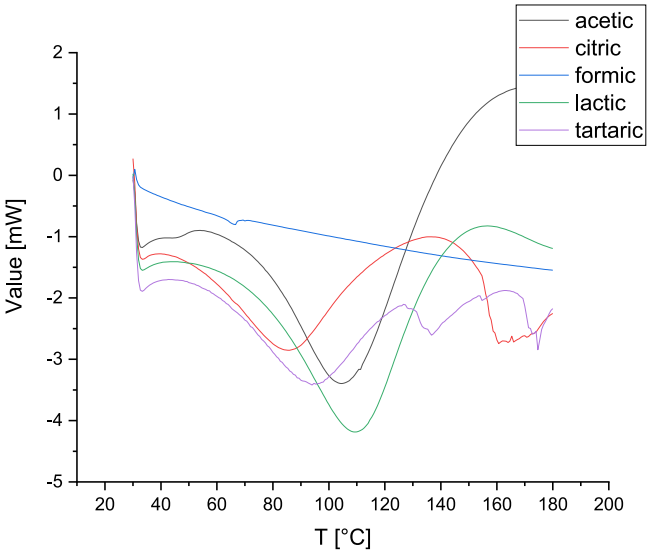

Fig. 7. DSC thermograms of chitosan thin films using different acid solvent during fabrication.

chitosan powder compared to the rest of the spectra, as it is corresponding to C═O stretching from carboxyl functional group (-COOH) of organic acids (i.e. citric, tartaric, acetic, lactic and formic acids), which were not present in chitosan powder.

X-ray diffraction (XRD) analysis of the thin films fabricated using different acids is presented in Fig. 6. All thin films made with five different acid solvents showed same peaks at 9° – 12°, known as plane (020), and 17° – 22°, known as plane (110) [42]. As the peaks were around 10° and 20°, the peaks of the thin films had inherited the peaks of the fungal chitosan powder. The diffraction peaks displayed by the thin

Table 4
Physical properties of pure chitosan thin films prepared using different acid solvent, from DSC and tensile strength analysis.

Acid solvent for chitosan thin film preparation	Glass transition temperature, *Tg* (°C)	Tensile strength (MPa)
Acetic acid	107.57	48.35 ± 0.00
Citric acid	78.01	6.28 ± 0.00
Formic acid	65.94	47.61 ± 5.45
Lactic acid	114.59	43.21 ± 0.00
Tartaric acid	87.36	4.55 ± 0.00

films indicated the hydrated conformation of chitosan [21]. XRD of the thin films showed broad peak at plane (110), showing that the thin films possessed amorphous diffraction pattern due to the presence of -NH_2 and -OH group [40,43]. Thin films fabricated using formic acid showed the highest crystallinity index (96.9%). With higher crystallinity, total dipole moment occurred as stresses being applied would create high piezoelectric coefficient [1,44].

Physical properties of pure chitosan thin films were characterized using differential scanning calorimetry (DSC) and tensile strength, DSC was used to measure the glass transition temperature (*Tg*) (Fig. 7). The dry state of chitosan was reported to show *Tg* at 203°C [45,46]. Table 4 presents *Tg* of pure chitosan thin films, where formic acid gave lowest *Tg* while using lactic acid would give highest *Tg* among the acid solvents used. Compared to the chitosan in dry state, *Tg* for chitosan prepared with any acids were acceptable as it can enter rubber state easier. Using temperatures that are lower than *Tg* would cause the material to be in glass state, which will lead to brittle film. Chitosan thin films using formic acid would easily be fabricated to possess a rubber-like state compared to the other thin films. This is desirable for the use of chitosan for wearable piezoelectric application.

The tensile test was done on pure chitosan thin films to investigate the effect of different acid solvents on the mechanical strength of the films. Table 4 depicts the tensile strength of pure chitosan thin films, where thin films prepared using acetic acid and formic acid exhibited the highest tensile strength compared to the other acid solvents. This could be due to the acetate ($H_3C_2OO^-$) and formate ($HCOO^-$) ions did not disrupt the chain of chitosan as aggressively as the other acids. Concentration and type of acid were reported to influence the topological limitations and density of the thin films, due to the presence of residual acid in the film [47,48]. Chitosan film prepared using citric acid was reported to possessed the lowest tensile strength compared to lactic and acetic acids [21], in accordance with the results obtained in this study. This is because citrate ions can react more strongly with chitosan and lead to the destruction of the interchain and intrachain hydrogen bonds in chitosan [21]. Thus, this led to the lowering of mechanical strength as being exhibited by the citric acid chitosan thin films [21]. Other study showed tensile strength of chitosan film with lactic acid solvent has significantly (P value$<$ 0.05) lower than that with formic, acetic, and propionic acids across all pH ranges [47]. The lower tensile strength of lactic acid could be due to its composition of one hydroxyl group instead of hydrogen in the structure compared with formic, acetic and propionic acids, which induced electrolyte instability in the solutions [47].

Among five acid solvents used, formic acid is among the best solvent as the thin film would return to its original state when the stress being applied on the material were removed, with the condition that the stress applied did not exceed the tensile strength. As piezoelectric materials are always subjected to mechanical stress and vibrations, it is important that the thin films can withstand the applied force to be used in piezoelectric application. Apart from possessing the highest tensile strength, chitosan thin film fabricated using formic acid showed the highest crystallinity index, which is favorable for piezoelectric application.

3.4. *Effect of different acid solvents on electrical properties of chitosan thin film*

The fabricated pure chitosan thin films prepared with different acid solvents were evaluated for its electrical properties using mechanical quality factor, Q_m, based on Eq. 2 and dissipation factor, tan δ, based on Eq. 3. The measurement of Q_m and tan δ was taken at 100 Hz as presented in Fig. 8. The reading of Q_m and tan δ at higher frequency showed lower Q_m and higher tan δ, making it undesirable in piezoelectric application. Low tan δ is a desirable characteristic for piezoelectric application [49]. This indicates that chitosan is suitable to be used low-frequency vibration piezoelectric sensor.

The results showed that when the thin films were fabricated using formic acid, Q_m is the highest and tan δ is the lowest, in comparison to acetic, lactic, citric and followed by tartaric acids. This attribute could be due to the solubility of the chitosan powder in the acid used, where the solubility of chitosan in the acids resulted in the crystallinity of the chitosan produced and the protonation of amino-groups [50,51]. The presence of free amino groups in chitosan are considered to be a strong base with a *pKa* value of 6.3, where at a pH of below 6 as the amines are protonated and renders chitosan to be readily soluble in dilute aqueous

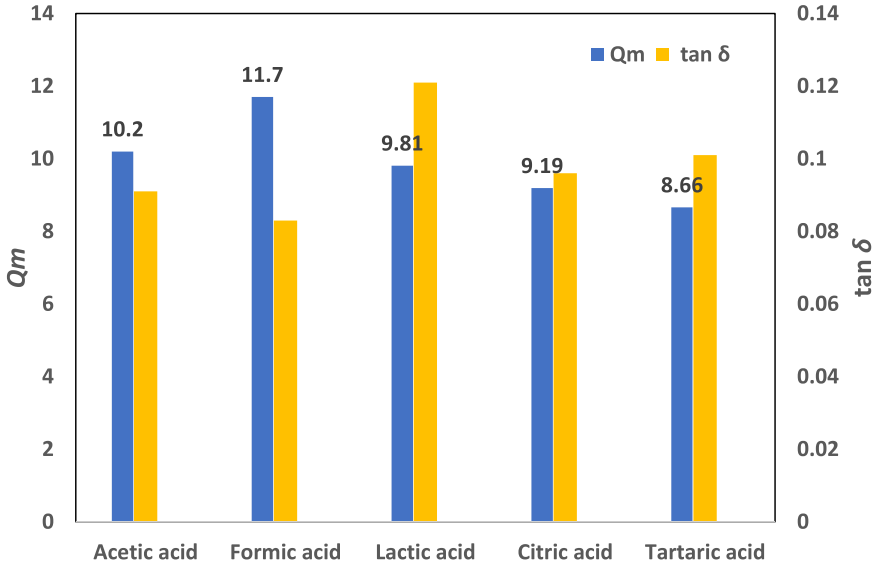

Fig. 8. The effect of the application of different acid solvents in the preparation of pure chitosan films on mechanical quality factor, Q_m and dissipation factor, tan δ of the thin films.

Table 5
Biodegradability test of pure chitosan thin films prepared using formic acid solvent, where the films were placed in four different conditions.

Thin films treatment	Weight loss after one month (%)
Submerged in water (Control)	0
Buried in soil	8.19
Buried in soil mixed with EM	100
Submerged in EM	100

acids [9,52]. Different acids used influenced the formation of counterion, where chitosan acted as polyelectrolyte, due to protonation of the amide ($-NH_2$) group, which allows its solubilization in organic acid solutions [53]. In organic acids (-COOH), amino groups first bind dissociated hydrogen ions, where after complete protonation of available H^+, chitosan begins interacting with undissociated acid molecules that creates a complex structure through ion cross-linking bonds between protonated amino groups and carboxylic acids [54,55]. The degree of protonation affects conductivity differently depending on acid type, where formic acid has higher protonation efficiency than acetic acid provides 3.6 times more H^+ ions for chitosan protonation. Higher protonation leads to stronger chitosan-acid interactions, promoting chain entanglement [54]. Formic acid has the lowest *pKa* value (3.75) and highest dissociation constant, *Ka* (1.77×10^{-4}) among acetic acid (4.76 and 1.8×10^{-5} respectively) and lactic acid (3.86 and 1.38×10^{-5} respectively).

This study demonstrated that formic acid is much more suitable to be used in solubilizing the chitosan during fabrication of thin film. It is preferrable for thin films to have higher Q_m and lower tan δ, making it suitable to be used as sensors [56]. The outcome of this study on electrical properties of formic acid-based chitosan thin film is comparable to other study, which discovered that chitosan film prepared using formic acid has higher piezoelectric coefficient (d_{31} and d_{33}) than that using acetic acid and lactic acid at 1.1 and 10 pC/N respectively, as well as higher electromechanical coupling factor [9]. Therefore, based on physical, chemical and electrical properties of pure chitosan thin films prepared using different acid solvents, formic acid was chosen for further study on chitosan thin films.

3.5. *Biological properties of pure chitosan thin film: biodegradability and anti-microbial activity*

Previous analysis pure chitosan thin films demonstrated that the film prepared using formic acid solvent resulted on superior mechanical and electrical properties. Formic acid-based pure chitosan thin film was evaluated for its biological properties through biodegradability and anti-microbial activity test. Table 5 presents the percent weight loss of thin films after one month in various conditions for biodegradability test. Thin films that are submerged in EM were observed to be the first one to completely dissolved, followed by the one that are buried in the soil mixed with EM. Various microorganisms that are present in the EM solution, such as lactic acid bacteria, yeasts and phototrophic bacteria, proved to help the degradation of thin films as the thin films being

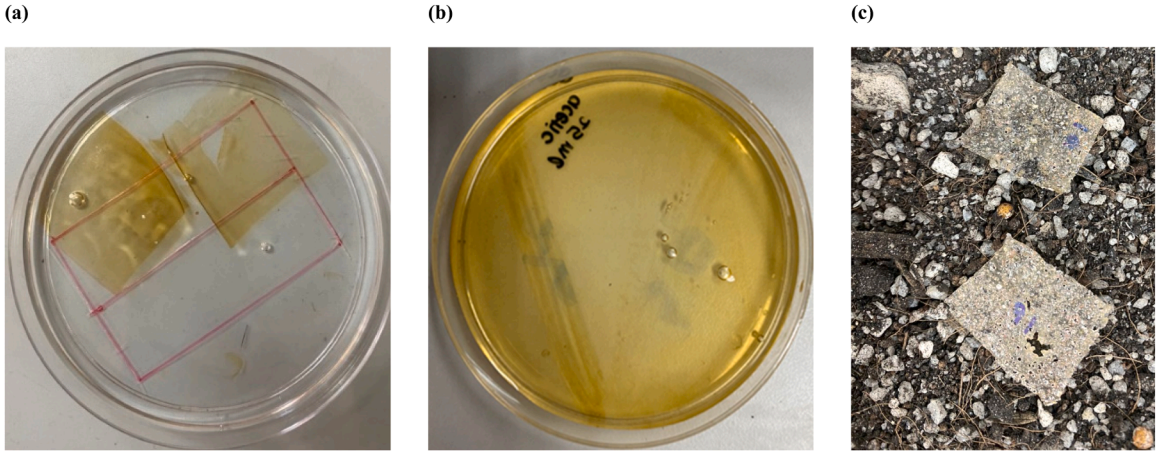

Fig. 9. Physical appearance of formic acid-based pure chitosan thin films from biodegradability test in different conditions after a month, which are (a) submerged in water (Control), (b) submerged in EM and (c) buried in soil after a month.

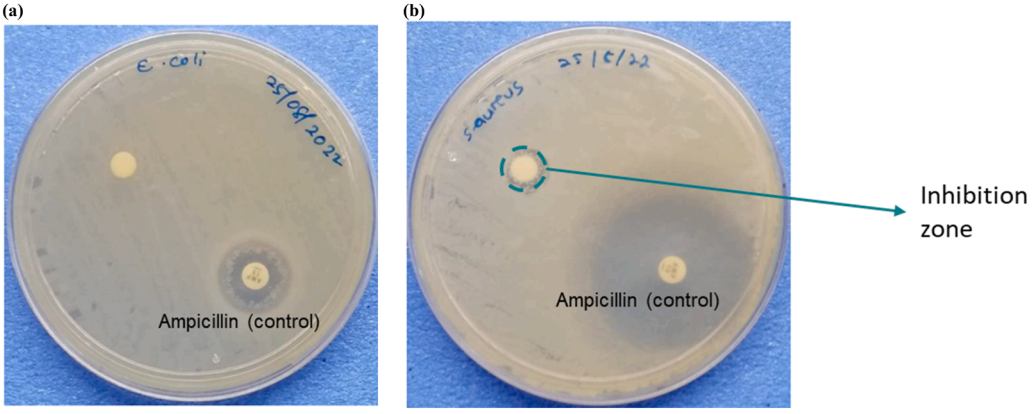

Fig. 10. The appearance of inhibition zone from anti-microbial test of pure chitosan thin films prepared using formic acid that is subjected to the bacteria colony of (a) *Escherichia coli* (gram negative) and (b) *Staphylococcus aureus* (gram positive). Ampicillin is used as control with (a) 12 mm and (b) 36 mm inhibition zone.

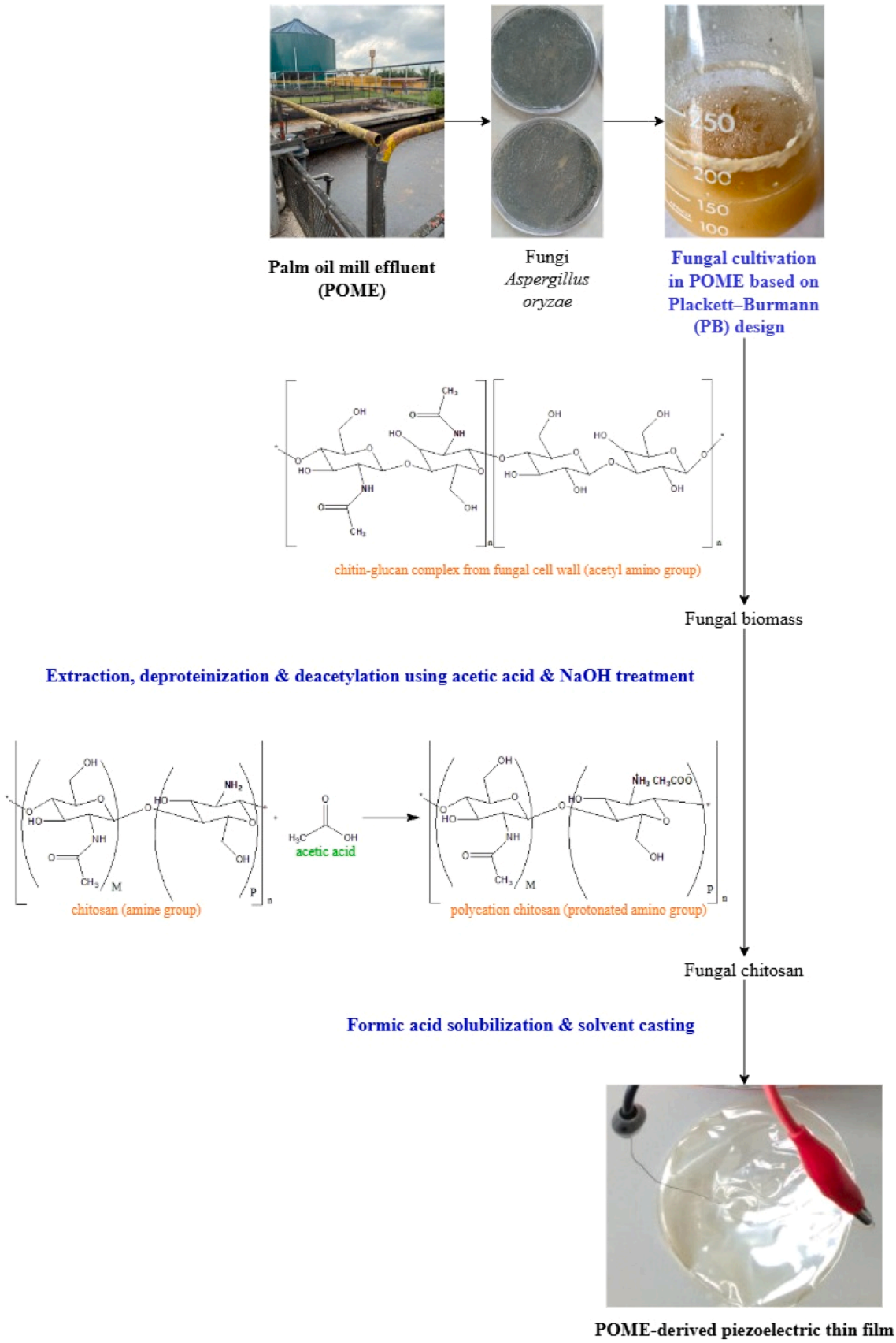

Fig. 11. Overview of fabrication POME-derived fungal chitosan thin film from the use of POME wastewater as the medium for the cultivation of fungi, where the harvested fungal biomass was subjected to extraction and deacetylation of chitin, followed by solvent casting of chitosan, for potential application in piezoelectric.

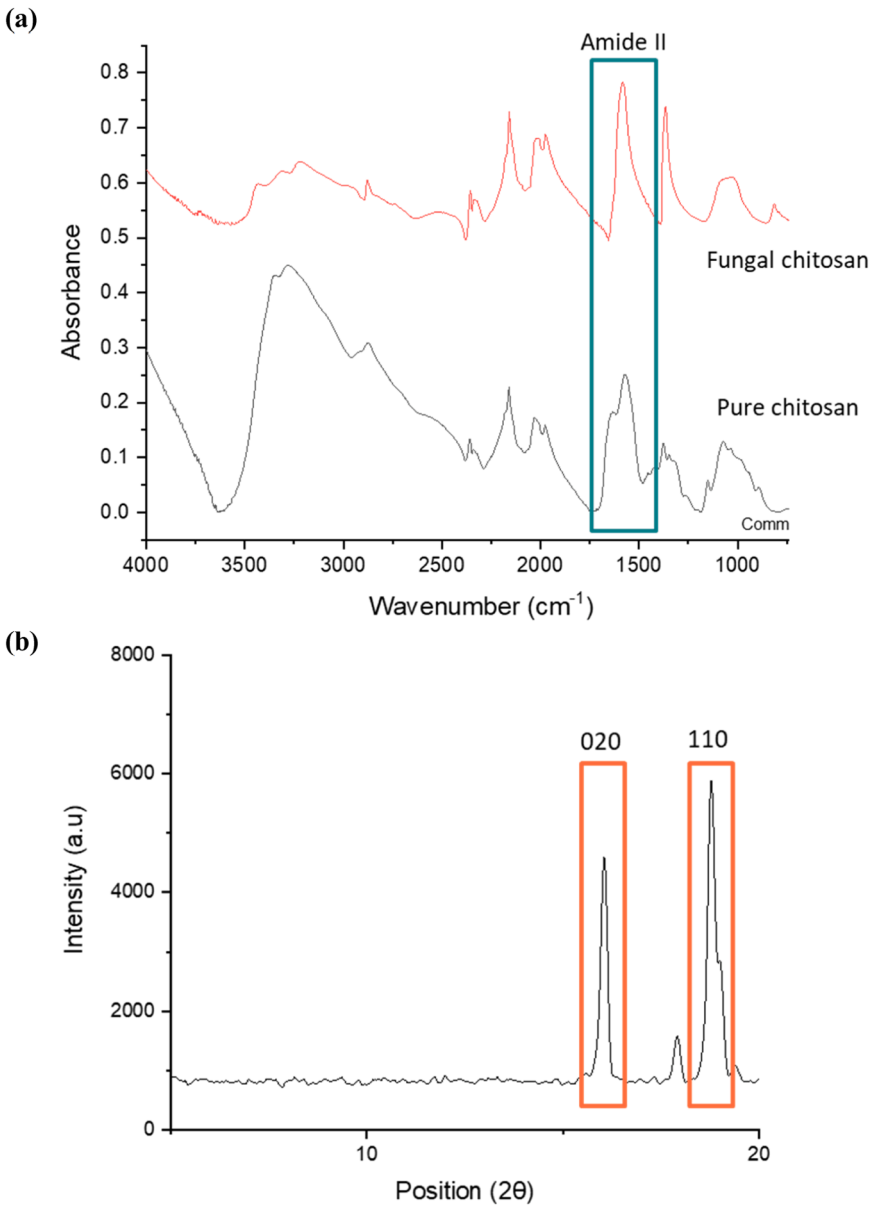

Fig. 12. (a) FTIR spectra and (b) XRD spectra of POME-derived fungal chitosan thin film.

buried in normal soil did not degrade as much. Fig. 9 shows observation on the physical appearance of the thin films after one month. The biodegradability test shows that chitosan thin films are biodegradable. The biodegradability of the thin films could be related to the crystallinity of the chitosan, where degradation occurred more favorably in amorphous regions compared to crystalline structure [57,58]. As water is an important element in microbial growth, better diffusion of water molecules into the amorphous part of the polymer would allow the increase in microbial degrading activity and microbial attack on the amorphous part [58]. This could explain low degradation of chitosan thin film as it possesses high crystallinity, which consequently makes chitosan thin films suitable to be used as wearable piezoelectric application.

Other polymeric piezoelectric thin films, such as PVDF, are non-biodegradable [2,59]. The degradation of PVDF film could be hazardous to the environment and human health due to the release of toxic substances [59]. In contrast, chitosan thin film demonstrated biodegradable characteristics where it would degrade once buried the soil, which could reduce the detrimental effect of e-waste abundance to the environment.

Anti-microbial activity test on chitosan thin film was performed using *Escherichia coli* and *Staphylococcus aureus,* two species of Gram-negative and Gram-positive bacteria respectively. These bacteria are pathogenic microorganisms responsible for diseases such as skin and strong bloodstream infections [26]. Ampicillin, an antibiotic, was used as the control in the antimicrobial test since ampicillin has the Gram-positive inhibition activity with increased Gram-negative inhibition activity, due to their ability to penetrate the outer membrane of gram-negative bacteria [60,61]. The anti-microbial activity test on the thin films resulted on the formation inhibition zone with the diameter of 6.0 ±0.0 mm for *E. coli* culture and 8.3 ±2.1 mm for *S. aureus* culture (Fig. 10). Chitosan was reported to possessed antimicrobial activity, which could be due to electrostatic interactions between the NH_3^+ sites of chitosan (positively charged) and the negatively charged membranes of microbial cells that alters the permeability of the microbial cell, causing the release of intracellular material [62]. The disruption of cell structure of *E. coli* and *S. aureus* in the interaction with chitosan was reported due to the binding of chitosan to microbial enzymes and nucleotides, as well as interaction of polycationic chitosan with negatively charged microbial surfaces that causes membrane disruption and the leakage of

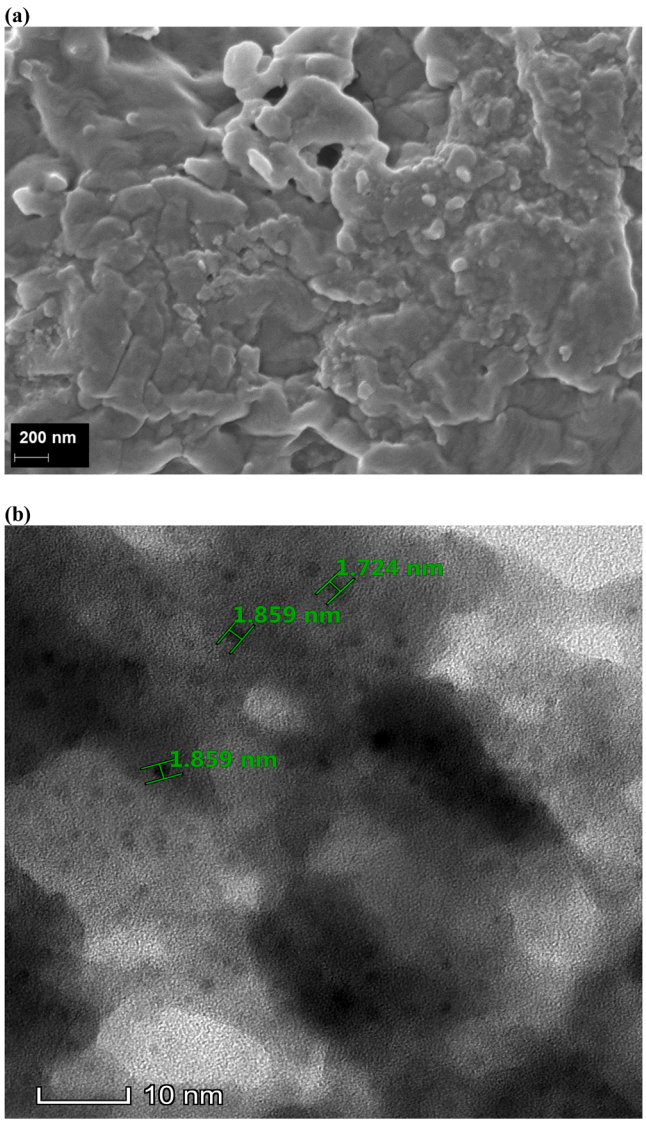

Fig. 13. Analysis of (a) FESEM (magnification 30,000 ×) and (b) TEM on POME-derived fungal chitosan thin film.

cellular components [63,64]. Therefore, the present of chitosan in the thin films could suppress the growth of bacteria that are common for skin infection, which increase its suitability to be used as wearable piezoelectric application.

3.6. Fabrication and characterization of POME-derived fungal chitosan thin film

As previous analysis shows that chitosan thin film prepared using formic acid solvents exhibited excellent properties for piezoelectric application, the fabrication of POME-derived fungal chitosan thin film was carried out using formic acid (Fig. 11). Chitosan was extracted from fungal biomass using organic acid treatment and alkaline treatment (Fig. 11), which involves removal of *B*-glucan from fungal biomass, deproteinization of chitin and deacetylation of chitin into chitosan [8,10]. The chemical, physical and electrical properties of the POME-derived fungal chitosan thin films were investigated for potential application in piezoelectricity.

Fig. 12(a) shows the FTIR spectra of commercially derived pure chitosan thin films and POME-derived fungal chitosan thin film. The absorption band for pure chitosan thin film appeared along 3000–3600 cm^{-1} and amide II band at 1481 cm^{-1}. However, the amide II band for fungal chitosan thin films shifted to 1420 cm^{-1}, which is lower than pure chitosan thin films. This finding established that the interaction between fungal chitosan with formic acid was weaker than the interaction between pure chitosan with formic acid. This could be due to the difference between DDA of the fungal chitosan (~82.57%) with pure chitosan (97.18%) that influenced the dissolution of chitosan in acid [10,21]. XRD spectra of POME-derived fungal chitosan thin film (Fig. 12(b)) shows similar planes as chitosan thin films that have been fabricated previously in Fig. 6, with peaks at plane (020) and plane (110). DDA of formic acid-based pure chitosan thin film is 97.18%. High DDA values indicates that more acetyl group has been removed from the fungal chitosan extracted. Fungal chitosan was reported to have lower DDA [10]. The surface morphology of the POME-derived fungal chitosan thin film from FESEM analysis (Fig. 13(a)) shows smoother surface and less flaky surface. From TEM analysis, the average particle size obtained was 1.814 nm ± 0.08 (Fig. 13(b)). This demonstrates that the POME-derived fungal chitosan thin film is a nanomaterial biopolymer.

The surface roughness of the POME-derived fungal chitosan thin film was analyzed using PFM (Fig. 14(a)). The root mean square roughness (R_q) obtained was 7.180 nm. The topographical analysis of the film is comparable to the root mean squared height of pure chitosan thin film by Amran et al. at 17.3 nm [9]. The surface roughness value indicates that the chitosan thin film had a smooth surface, which is critical for piezoelectric material, to prevent current leakage and a low dielectric constant [9,65]. Current leakage and low dielectric constant could lead to low piezoelectric coefficient [9,65]. The impact of surface roughness on electrical conductivity is through the alteration of the area of contact and the path which electrons travel, where a completely smooth and flat surface would allow for uniform electron flow with minimal resistance [66]. Surface roughness reduces the admittance and phase values of resonators, where the positive and negative charges generated by the piezoelectric effect cannot be completely balanced on rough surface [67]. This leads to the generation of ripples in the admittance and phase values, which is not conducive to the operation of resonators in the circuit [67]. The fundamental principle of PFM is the converse piezoelectric effect, where a piezoelectrically active material undergoes deformation upon the application of an electric field [1,68]. Fig. 14(b-d) presents PFM phase, PFM amplitude and surface potential of POME-derived fungal chitosan thin film, respectively. Fig. 14(b) displays noisy phase image, which confirms that the crystalline regions in chitosan biopolymer are piezoelectric but non-ferroelectric. The bright yellow and white flecks from Fig. 14(c) shows regions with a strong piezoelectric response, with up to 30.2 pm of displacement. The amplitude image visualizes the physical magnitude of the piezoelectric response, due to the expansion and contraction of materials when an electrical voltage is applied by the microscope tip [69,70]. From Fig. 14 (d), the bright yellow and white spots scattered across the image correspond to 10–14.4 mV, represent highly localized, discrete regions that exhibit a strong piezoelectric effect attributed by high electromechanical coupling. From PFM analysis, at the highest amplitude of the electromechanical strain obtained, effective piezoelectric coefficient (d_{eff}) of the POME-derived fungal chitosan thin film is 6.04 pm/V (dimensional unity with pC/N). However, these PFM images indicated that the film regions were mainly heterogenous, which could lead to poor piezoelectricity. Optimising fabrication parameters of chitosan thin film from POME-derived fungal biomass could improve homogeneity of piezoelectric chitosan film in future studies.

The electrical properties, Q_m and tan δ of thin films fabricated from POME-derived fungal chitosan thin film (11.9 and 0.083, respectively) revealed similar results to the pure chitosan thin films from Fig. 8. This finding demonstrates that formic acid is the most suitable solvent even for fungal chitosan, as the values from the electrical properties were in agreement with that of pure chitosan thin films. However, the Q_m of the PVDF thin films were reported to be higher than chitosan thin films at 17.2 [71]. The slightly lower Q_m of chitosan thin film is due to the low crystallinity of the extracted fungal chitosan, where the crystallinity of

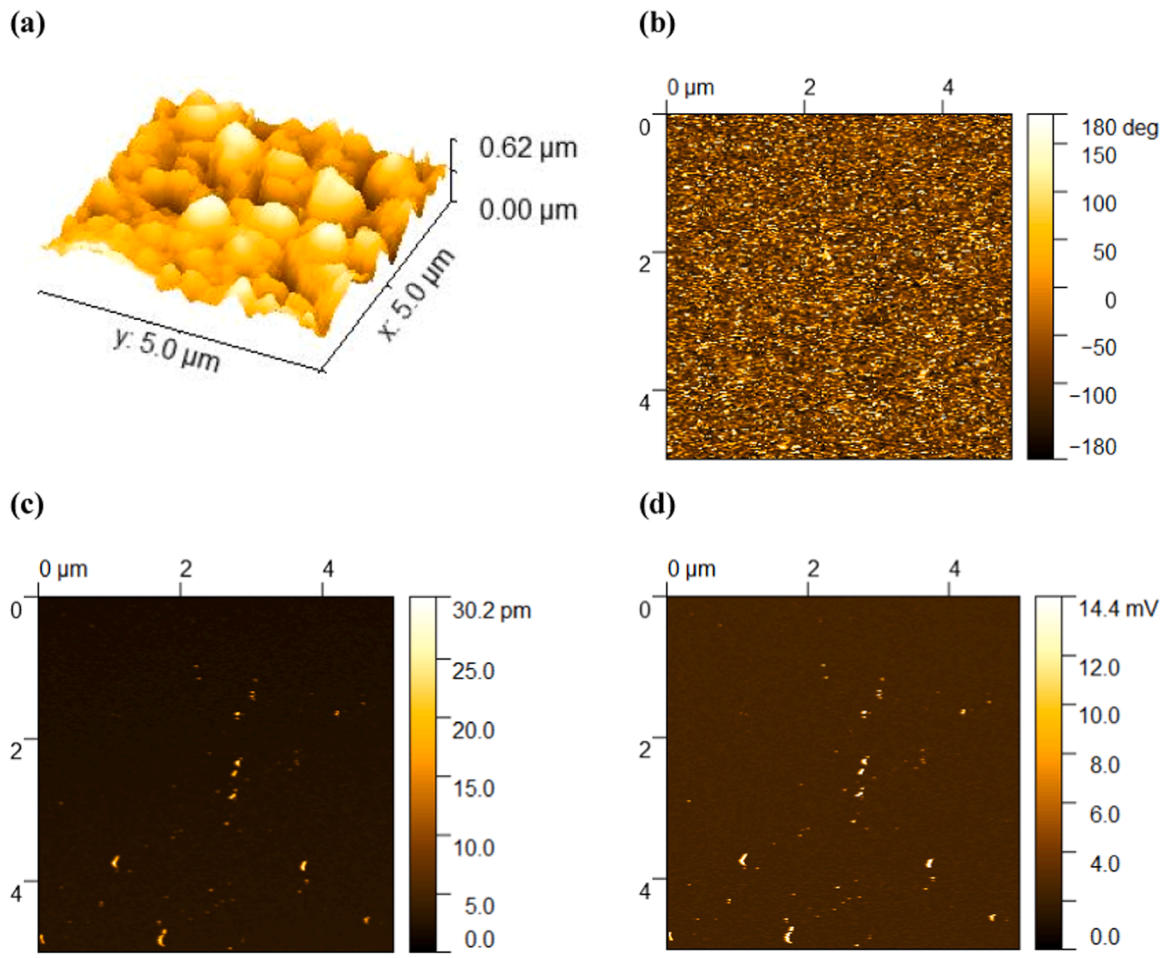

Fig. 14. (a-d) PFM on POME-derived fungal chitosan thin film.

the material would influence the dipole moment occurred [44]. The application of POME-derived fungal chitosan thin film as piezoelectric material is promising as it possesses high Q_m and low tan δ, which renders the energy loss from piezoelectric material to be minimal. Therefore, this study reveals that piezoelectric biomaterial could be fabricated sustainability from agro-industrial waste through fungal cultivation and chitosan extraction.

Due to its mechanical strength, flexibility and biocompatibility, POME-derived fungal chitosan film is suitable for the application of free-standing wearable piezoelectric sensor. The application of POME-derived fungal chitosan film in piezoelectric application could support biorefinery of palm oil processing, which subsequently improve sustainability and circular bioeconomy of palm oil industry. The use of POME in the fabrication of piezoelectric chitosan thin film also has the potential to enhance sustainability of electronic devices production in comparison to the use of conventional synthetic polymers and ceramics. Using biodegradable materials, like POME-derived fungal chitosan film in bioelectronics would assist in lessening environmental impact from e-waste disposal.

4. Conclusion

This study reports novel use of POME-derived *A. oryzae* biomass for the fabrication of fungal chitosan thin film as piezoelectric biomaterial. Screening of cultivation medium for fungal cultivation using PB design showed that the medium supplemented with POME has the highest yield with minimal nutrients and no addition of glucose as the carbon source. The fungal cultivation has reduced COD of POME by 37%, indicated that this process is promising for POME bioremediation. Acetic acid, formic acid, citric acid, tartaric acid and lactic acid was employed in the investigation of organic acid solvents effect on chitosan thin film fabrication. Formic acid chitosan thin film was shown to have superior tensile strength and crystallinity index, as well as the best electrical properties with the largest Q_m and the lowest tan δ, which is favorable for piezoelectric application. Formic acid chitosan thin film was also demonstrated its biodegradability, which make it safer for the environment. The film also exhibited antimicrobial properties, which make it favourable as wearable piezoelectric device. Fungal chitosan was extracted from the cultivation on POME for the fabrication of thin film using formic acid as solvent. POME-derived fungal chitosan film showed promising electrical properties with d_{eff} of 6.04 pm/V, Q_m of 11.9 and tan δ of 0.083. The use of POME in the fabrication of piezoelectric thin film has the potential to improve sustainability of the palm oil industry and electronic devices production.

CRediT authorship contribution statement

MH Maziati Akmal: Formal analysis, Methodology, Supervision, Validation, Resources, Software. **Ahmad Farah:** Writing – review & editing, Visualization, Validation, Supervision, Resources, Project administration, Methodology, Funding acquisition, Formal analysis, Data curation, Conceptualization. **Hazmi Alia Tasnim:** Formal analysis, Investigation, Methodology, Visualization, Writing – original draft, Data curation. **Ali Fathilah:** Supervision. **Md Ralib Aliza Aini:** Formal analysis, Supervision, Validation.

Declaration of Competing Interest

The authors declare that they have no known competing financial interests or personal relationships that could have appeared to influence the work reported in this paper.

Acknowledgements

The authors acknowledge financial assistance from Ministry of Higher Education, Malaysia under Fundamental Research Grant Scheme (FRGS) (FRGS/1/2019/TK02/UIAM/02/3).

References

[1] M.H.M. Akmal, F.B. Ahmad, Bionanomaterial Thin Film for Piezoelectric Applications, in: A.T. Jameel, A.Z. Yaser (Eds.), Advances in Nanotechnology and Its Applications, Springer Singapore, Singapore, 2020, pp. 63–82.
[2] M.H. Maziati Akmal, et al., 16 - Biopolymer-based waste for biomaterials thin film in piezoelectric application, in: A. Khan, et al. (Eds.), Advanced Technology for the Conversion of Waste Into Fuels and Chemicals, Editors, Woodhead Publishing, 2021, pp. 355–381.
[3] H. Kaczmarek, et al., Advances in the study of piezoelectric polymers, Russ. Chem. Rev. 88 (7) (2019) 749.
[4] M.T. Chorsi, et al., Piezoelectric biomaterials for sensors and actuators, Adv. Mater. 31 (1) (2019) 1802084.
[5] A. Hänninen, et al., Nanocellulose and chitosan based films as low cost, green piezoelectric materials, Carbohydr. Polym. 202 (2018) 418–424.
[6] E. Praveen, S. Murugan, K. Jayakumar, Investigations on the existence of piezoelectric property of a bio-polymer–chitosan and its application in vibration sensors, RSC Adv. 7 (56) (2017) 35490–35495.
[7] F.B. Ahmad, et al., Characterization of chitosan from extracted fungal biomass for piezoelectric application, IOP Conf. Ser. Mater. Sci. Eng. 778 (2020) 012034.
[8] A.T. Hazmi, et al., Microbial chitosan for the fabrication of piezoelectric thin film, IOP Conf. Ser. Mater. Sci. Eng. 1173 (1) (2021) 012043.
[9] A. Amran, et al., Biosynthesis of thin film derived from microbial chitosan for piezoelectric application, Mater. Today Commun. 29 (2021) 102919.
[10] A.T. Hazmi, et al., Fungal chitosan for potential application in piezoelectric energy harvesting: Review on experimental procedure of chitosan extraction, Alex. Eng. J. 67 (2023) 105–116.
[11] A.Z. Athoillah, F.B. Ahmad, Biodiesel production from bioremediation of palm oil mill effluent via oleaginous fungi, Clean Soil Air Water 50 (4) (2022) 2200025.
[12] M. Kumaran, et al., Agriculture of microalgae Chlorella vulgaris for polyunsaturated fatty acids (PUFAs) production employing palm oil mill effluents (POME) for future food, wastewater, and energy nexus, Energy Nexus 9 (2023) 100169.
[13] F.B. Ahmad, et al., The outlook of the production of advanced fuels and chemicals from integrated oil palm biomass biorefinery, Renew. Sustain. Energy Rev. 109 (2019) 386–411.
[14] N.A. Osman, et al., The effect of palm oil mill effluent final discharge on the characteristics of pennisetum purpureum, Sci. Rep. 10 (1) (2020) 6613.
[15] A.H. Nour, N.H. Azhari, Y.M. Rosli, The Performance Evaluation of Anaerobic Methods for Palm Oil Mill Effluent (POME) Treatment: A Review, in: N.W.T. Quinn (Ed.), International Perspectives on Water Quality Management and Pollutant Control, IntechOpen, Rijeka, 2013.
[16] D. Dominic, S. Baidurah, A review of biological processing technologies for palm oil mill waste treatment and simultaneous bioenergy production at laboratory scale, pilot scale and industrial scale applications with technoeconomic analysis, Energy Convers. Manag. X (26) (2025) 100914.
[17] H. Kamyab, et al., Isolate new microalgal strain for biodiesel production and using FTIR spectroscopy for assessment of pollutant removal from palm oil mill effluent (POME), Chem. Eng. Trans. 63 (2018) 91–96.
[18] A. Hänninen, et al., Piezoelectric sensitivity of a layered film of chitosan and cellulose nanocrystals, Procedia Eng. 168 (2016) 1176–1179.
[19] K. Nilsson, J. Bjurman, Chitin as an indicator of the biomass of two wood-decay fungi in relation to temperature, incubation time, and media composition, Can. J. Microbiol. 44 (6) (1998) 575–581.
[20] Hach, Oxygen Demand, Chemical, 2009, Hach: Colorado.
[21] C. Qiao, et al., Structure and properties of chitosan films: effect of the type of solvent acid, Lwt 135 (2021) 109984.
[22] C.-H. Lin, P.-H. Wang, T.-C. Wen, Chitosan production from Paecilomyces saturatus using three monosaccharides via mixture design, Int. J. Biol. Macromol. 141 (2019) 307–312.
[23] Z. Butt, et al., Investigation of electrical properties & mechanical quality factor of piezoelectric material (PZT-4A), J. Electr. Eng. Technol. 12 (2) (2017) 846–851.
[24] R. Proksch, In-situ piezoresponse force microscopy cantilever mode shape profiling, J. Appl. Phys. 118 (7) (2015).
[25] S. Baidurah, et al., Evaluation of soil burial biodegradation behavior of poly(3-hydroxybutyrate-co-3-hydroxyhexanoate) on the basis of change in copolymer composition monitored by thermally assisted hydrolysis and methylation-gas chromatography, J. Anal. Appl. Pyrolysis 137 (2019) 146–150.
[26] M. Barbălată-Mândru, et al., Poly(vinyl alcohol)/Plant Extracts Films: Preparation, Surface Characterization and Antibacterial Studies against Gram Positive and Gram Negative Bacteria, Materials 15 (7) (2022) 2493.
[27] Support, M.Specify the design for Create Plackett-Burman Design. Statistical Modeling 2026 [cited 2026; Available from: ⟨https://support.minitab.com/en-us/minitab/help-and-how-to/statistical-modeling/doe/how-to/factorial/create-factorial-design/create-plackett-burman/create-the-design/specify-the-design/⟩.
[28] L. Flechner, T.Y. Tseng, Understanding results: P: -values, confidence intervals, and number need to treat, Indian J. Urol. 27 (4) (2011) 532–535.
[29] F.B. Ahmad, et al., Optimising extraction of microalgal oil using accelerated solvent extraction by response surface methodology, J. Eng. Sci. Technol. 13 (4) (2018) 964–976.
[30] L. Yan, et al., Improvement of tacrolimus production in Streptomyces tsukubaensis by mutagenesis and optimization of fermentation medium using Plackett–Burman design combined with response surface methodology, Biotechnol. Lett. 43 (9) (2021) 1765–1778.
[31] M.H. Hasni, F.B. Ahmad, A.Z. Athoillah, The production of microbial biodiesel from cellulose-derived fungal lipid via consolidated bioprocessing, Environ. Technol. Innov. 30 (2023) 103123.
[32] Stat-Ease, Version 6 User's Guide Design-Expert Software, Stat-Ease, Inc, 2000.
[33] B.G. Lopes, et al., Classification of the coefficient of variation for experiments with eucalyptus seedlings in greenhouse, Rev. Ciência Agron. ômica 52 (4) (2021) e20207587.
[34] K. Tafazzoli, M. Ghavami, K. Khosravi-Darani, Investigation of impact of siderophore and process variables on production of iron enriched Saccharomyces boulardii by Plackett–Burman design, Sci. Rep. 14 (1) (2024) 22813.
[35] X.-y Ma, et al., The effects of zinc sulfate on mycelial enzyme activity and metabolites of Pholiota adiposa, Plos One 18 (12) (2023) e0295573.
[36] C. Kang, et al., Biological characteristics of the mycelium and optimization of the culture medium for Phallus dongsun, Pol. J. Microbiol. 73 (2) (2024) 237–252.
[37] F.B. Ahmad, et al., Improved microbial oil production from oil palm empty fruit bunch by Mucor plumbeus, Fuel 194 (2017) 180–187.
[38] F.B. Ahmad, et al., A multi-criteria analysis approach for ranking and selection of microorganisms for the production of oils for biodiesel production, Bioresour. Technol. 190 (2015) 264–273.
[39] C. Uwineza, et al., Cultivation of edible filamentous fungus Aspergillus oryzae on volatile fatty acids derived from anaerobic digestion of food waste and cow manure, Bioresour. Technol. 337 (2021) 125410.
[40] H.Y.C.- Eulalio, et al., Characterization and thermal properties of chitosan films prepared with different acid solvents, Rev. Cuba. De. Química 31 (3) (2019) 309–323.
[41] PubChem. Formic Acid. [cited 2025; Available from: ⟨https://pubchem.ncbi.nlm.nih.gov/compound/Formic-Acid⟩.
[42] L. Cui, et al., Preparation and characterization of chitosan membranes, RSC Adv. 8 (50) (2018) 28433–28439.
[43] M. Eddya, B. Tbib, E.-H. Khalil, A comparison of chitosan properties after extraction from shrimp shells by diluted and concentrated acids. Heliyon 6 (2) (2020).
[44] M. Baniasadi, et al., Correlation of annealing temperature, morphology, and electro-mechanical properties of electrospun piezoelectric nanofibers, Polymer 127 (2017) 192–202.
[45] J. Tanigawa, N. Miyoshi, K. Sakurai, Characterization of chitosan/citrate and chitosan/acetate films and applications for wound healing, J. Appl. Polym. Sci. 110 (1) (2008) 608–615.
[46] M. Labardi, et al., Glass transition and crystallization of chitosan investigated by broadband dielectric spectroscopy, Polymers 17 (20) (2025) 2758.
[47] K.M. Kim, et al., Properties of chitosan films as a function of pH and solvent type, J. Food Sci. 71 (3) (2006) p. E119-E124.
[48] J. Xu, et al., Regulating the physicochemical properties of chitosan films through concentration and neutralization, Foods 11 (11) (2022) 1657.
[49] S. Bhattacharjee, et al., Dielectric and piezoelectric augmentation in self-poled magnetic Fe3O4/poly(vinylidene fluoride) composite nanogenerators, Mater. Res. Express 7 (4) (2020) 044001.
[50] I.A. Sogias, V.V. Khutoryanskiy, A.C. Williams, Exploring the factors affecting the solubility of chitosan in water, Macromol. Chem. Phys. 211 (4) (2010) 426–433.
[51] N. Pinpru, C. Ninthap, V. Intasanta, Crystallinity reconstruction of squid-pen chitosan into mechanically robust and multifunctional bionanocomposite food packaging film, ACS Omega 9 (40) (2024) 41179–41193.
[52] J.L. Chen, Y. Zhao, Effect of molecular weight, acid, and plasticizer on the physicochemical and antibacterial properties of β-chitosan based films, J. Food Sci. 77 (5) (2012) p. E127-E136.
[53] S.A. Salazar-Brann, et al., Electrospinning of chitosan from different acid solutions, AIMS Bioeng. 8 (1) (2021) 112–129.
[54] Q.-x Li, et al., Electrolytic conductivity behaviors and solution conformations of chitosan in different acid solutions, Carbohydr. Polym. 63 (2) (2006) 272–282.
[55] F. Araújo, et al., Effect of chitosan properties and dissolution state on solution rheology and film performance in triboelectric nanogenerators, Gels 11 (7) (2025) 523.
[56] H. Zu, H. Wu, Q.-M. Wang, High-temperature piezoelectric crystals for acoustic wave sensor applications, IEEE Trans. Ultrason. Ferroelectr. Freq. Control 63 (3) (2016) 486–505.
[57] M.J. Jenkins, K.L. Harrison, The effect of crystalline morphology on the degradation of polycaprolactone in a solution of phosphate buffer and lipase, Polym. Adv. Technol. 19 (12) (2008) 1901–1906.
[58] C. Lors, P. Leleux, C.H. Park, State of the art on biodegradability of bio-based plastics containing polylactic acid, Front. Mater. 11 (2025) **2024**.

[59] J. Li, et al., Degradable piezoelectric biomaterials for wearable and implantable bioelectronics, Curr. Opin. Solid State Mater. Sci. 24 (1) (2020) 100806.
[60] L.G. Winston, D. Deck, A.F. Bolger, in: S.A. Waldman, et al. (Eds.), CHAPTER 81 - ENDOCARDITIS, in Pharmacology and Therapeutics, Editors, W.B. Saunders, Philadelphia, 2009, pp. 1121–1140.
[61] N. Tarannum, S. Khatoon, B.B. Dzantiev, Perspective and application of molecular imprinting approach for antibiotic detection in food and environmental samples: a critical review, Food Control 118 (2020) 107381.
[62] A. Guarnieri, et al., Antimicrobial properties of chitosan from different developmental stages of the bioconverter insect Hermetia illucens, Sci. Rep. 12 (1) (2022) 8084.
[63] Y.-C. Chung, C.-Y. Chen, Antibacterial characteristics and activity of acid-soluble chitosan, Bioresour. Technol. 99 (8) (2008) 2806–2814.
[64] J. Laanoja, et al., Particle-driven synergistic antibacterial effect of silver–chitosan nanocomposites against Escherichia coli, Pseudomonas aeruginosa, and Staphylococcus aureus, ACS Omega 10 (26) (2025) 27904–27919.
[65] M.A.M. Harttar, M.W.A. RASHID, U.A.A. Azlan, Physical and electrical properties enhancement of rare-earth doped-potassium sodium niobate (KNN): a review, Ceram. Silik. áty 59 (2) (2015) 158–163.
[66] ProPlate. The Impact of Surface Roughness on Electrical Conductivity in Metal Plating Processes. 2025; Available from: ⟨https://www.proplate.com/how-do-factors-like-surface-roughness-achieved-after-metal-plating-affect-electrical-conductivity/⟩.
[67] M. Li, et al., Surface roughness effects on the vibration characteristics of AT-cut quartz crystal plate, Sensors 23 (11) (2023) 5168.
[68] P. Buragohain, et al., Quantification of the electromechanical measurements by piezoresponse force microscopy, Adv. Mater. 34 (47) (2022) 2206237.
[69] P. Sharma, et al., Orientational imaging in polar polymers by piezoresponse force microscopy, J. Appl. Phys. 110 (5) (2011).
[70] S.M. Neumayer, et al., Piezoresponse amplitude and phase quantified for electromechanical characterization, J. Appl. Phys. 128 (17) (2020).
[71] J. Song, et al., Design optimization of PVDF-based piezoelectric energy harvesters, Heliyon 3 (9) (2017) e00377.